THE JOURNAL OF BIOLOGICAL CHEMISTRY
Vol. 279, No. 43, Issue of October 22, pp. 44384–44393, 2004
Printed in U.S.A.
© 2004 by The American Society for Biochemistry and Molecular Biology, Inc.

The Iron Superoxide Dismutase from the Filamentous Cyanobacterium *Nostoc* PCC 7120

LOCALIZATION, OVEREXPRESSION, AND BIOCHEMICAL CHARACTERIZATION*

Received for publication, June 4, 2004, and in revised form, July 28, 2004
Published, JBC Papers in Press, August 9, 2004, DOI 10.1074/jbc.M406254200

Günther Regelsberger‡, Ulrike Laaha‡, Dagmar Dietmann‡, Florian Rüker§, Antonella Canini¶, Maria Grilli-Caiola¶, Paul Georg Furtmüller‡, Christa Jakopitsch‡, Günter A. Peschek‖, and Christian Obinger‡

From the ‡Department of Chemistry, Division of Biochemistry, Metalloprotein Research Group, BOKU, University of Natural Resources and Applied Life Sciences, Muthgasse 18, A-1190 Vienna, Austria, the §Department of Biotechnology, BOKU, University of Natural Resources and Applied Life Sciences, Muthgasse 18, A-1190 Vienna, Austria, the ¶Department of Biology, University of Rome Tor Vergata, Via della Ricerca Scientifica 1, I-00133 Rome, Italy, and the ‖Institute of Physical Chemistry, Molecular Bioenergetics Group, University of Vienna, Althanstrasse 14, A-1090 Vienna, Austria

The nitrogen-fixing filamentous cyanobacterium *Nostoc* PCC 7120 (formerly named *Anabaena* PCC 7120) possesses two genes for superoxide dismutase, a unique membrane-associated manganese superoxide dismutase (MnSOD) and a soluble iron superoxide dismutase (FeSOD). A phylogenetic analysis of FeSODs shows that cyanobacterial enzymes form a well separated cluster with filamentous species found in one subcluster and unicellular species in the other. Activity staining, inhibition patterns, and immunogold labeling show that FeSOD is localized in the cytosol of vegetative cells and heterocysts (nitrogenase containing specialized cells formed during nitrogen-limiting conditions). The recombinant *Nostoc* FeSOD is a homodimeric, acidic enzyme exhibiting the characteristic iron peak at 350 nm in its ferric state, an almost 100% occupancy of iron per subunit, a specific activity using the ferricytochrome assay of (2040 ± 90) units mg^{-1} at pH 7.8, and a dissociation constant K_d of the azide-FeSOD complex of 2.1 mM. Using stopped flow spectroscopy it was shown that the decay of superoxide in the presence of various FeSOD concentrations is first-order in enzyme concentration allowing the calculation of the catalytic rate constants, which increase with decreasing pH: 5.3×10^9 M^{-1} s^{-1} (pH 7) to 4.8×10^6 M^{-1} s^{-1} (pH 10). FeSOD and MnSOD complement each other to keep the superoxide level low in *Nostoc* PCC 7120, which is discussed with respect to the fact that *Nostoc* PCC 7120 exhibits oxygenic photosynthesis and oxygen-dependent respiration within a single prokaryotic cell and also has the ability to form differentiated cells under nitrogen-limiting conditions.

Cyanobacteria are oxygenic, phototrophic prokaryotes combining the mechanisms of plant-type photosynthesis and cytochrome *c* oxidase-based respiration in one cell (1). Because the cyanobacteria were the first organisms that produced molecular oxygen they necessarily had to find a way to balance between death and life, because in aerobic organisms active oxygen species such as superoxide radicals, hydroxyl radicals, and hydrogen peroxide are inevitably formed. For the efficient removal of reactive oxygen species the cyanobacteria, as well as other organisms, developed quite a number of strategies including redox enzymes such as superoxide dismutases (SODs).[1] Genome analysis (www.kazusa.or.jp/cyano/cyano.html) shows that cyanobacteria possess either one or more SOD genes encoding SODs with iron, manganese, copper-zinc, or nickel at the active site (2).

The filamentous, nitrogen-fixing cyanobacterium *Nostoc* PCC 7120 (formerly named *Anabaena* PCC 7120) was recently shown to contain two genes for SODs, namely a *sodB* gene encoding an iron-containing and a *sodA* gene encoding a manganese-containing superoxide dismutase (2). *Nostoc* PCC 7120 forms heterocysts when the filaments are grown under nitrogen-limiting conditions (3). Mature heterocysts are the site of nitrogen fixation and contain nitrogenase, the enzyme that catalyzes the reduction of atmospheric nitrogen to ammonia. Because nitrogenase is irreversibly inhibited upon exposure to molecular oxygen or activated oxygen species (4), several strategies are necessary to protect this ancient enzyme: (i) heterocysts have no oxygen-evolving activity because they lack photosystem II (4), (ii) they are surrounded by a thick cell wall (5), and (iii) they have a high activity of respiration which consumes oxygen (6). In nonheterocyst nitrogen-fixing cyanobacteria, nitrogen fixation and oxygenic photosynthesis are separated temporally or spatially (7).

The protection mechanism in heterocysts is not perfect. The thick cell wall does not totally exclude oxygen penetration into the cells (5), and both the respiratory electron transport and photosystem I contribute to the formation of superoxide radicals (4). Thus, superoxide dismutase activity is necessary in both vegetative cells and heterocysts of cyanobacteria in order to protect against cellular damage by superoxide. We have reported that *Nostoc* PCC 7120 MnSOD is unique in being membrane-bound and presented a comprehensive biochemical and biophysical characterization of this enzyme (2). MnSOD is

* This work was supported by the Austrian Science Fund (FWF-Project P13069-CHE). The costs of publication of this article were defrayed in part by the payment of page charges. This article must therefore be hereby marked "*advertisement*" in accordance with 18 U.S.C. Section 1734 solely to indicate this fact.

** To whom correspondence should be addressed. Fax: 43-1-36006-6059; E-mail: christian.obinger@boku.ac.at.

[1] The abbreviations used are: SOD, superoxide dismutase; CM, cytoplasmic or plasma membrane; DMF, dimethylformamide; FeSOD, iron-containing superoxide dismutase; ICM, intracytoplasmic or thylakoid membrane; MnSOD, manganese-containing superoxide dismutase; PCC, Pasteur Culture Collection; PMSF, phenylmethylsulfonyl fluoride; Pipes, 1,4-piperazinediethanesulfonic acid; PBS, phosphate-buffered saline.

This paper is available on line at http://www.jbc.org

Downloaded from http://www.jbc.org/ by guest on July 25, 2018

localized in both cytoplasmic and thylakoid membranes (2). Recently, the 2.0-Å structure of the catalytic portion of the MnSOD was reported (8). Membrane attachment of *Nostoc* MnSOD was confirmed by immunoblotting and activity staining (9).

To complete the characterization of SODs in *Nostoc* PCC 7120 and understand superoxide detoxification in nitrogen-fixing heterocystous cyanobacteria, we cloned the *sodB* gene from this organism and performed a comprehensive biochemical and kinetic investigation including the determination of actual bimolecular rate constants at pH 7–10. Its localization in the cytosol of both vegetative cells and heterocysts is presented as well as its phylogenetic relationship with other cyanobacterial FeSODs. Comparing these findings with those from MnSOD obtained under identical experimental conditions, we conclude that FeSOD and MnSOD complement each other in *Nostoc* PCC 7120 to protect cell components from oxidative stress. The physiological relevance is discussed with respect to the bioenergetic peculiarities of cyanobacteria as well as to nitrogen fixation in heterocysts. The SOD equipment of *Nostoc* PCC 7120 is compared with that of other cyanobacteria.

EXPERIMENTAL PROCEDURES

Materials

Enzymes and chemicals were used from the following companies: alkaline phosphatase from Roche Applied Science; T4 DNA ligase, NcoI and XhoI restriction enzymes from MBI Fermentas; ExTaq DNA polymerase from TaKaRa; Epoxy resin kit from Multilab; bovine serum albumin, lysozyme (from chicken egg white), DNase I (from bovine pancreas), PMSF, leupeptin, pepstatin A, fibrinogen type IV (from bovine plasma), thrombin (from bovine plasma), SigmaMarker (wide molecular weight range), electrophoresis kit for isoelectric focusing, cytochrome *c* (from horse heart), xanthine, xanthine oxidase (from buttermilk grade I), 18-crown-6-ether, 3-Å molecular sieve and potassium superoxide from Sigma; the GFX PCR DNA and gel band purification kit, gel filtration LMW calibration kit, chelating Sepharose fast flow, Superdex 200 prep grade, and PD-10 desalting columns from Amersham Biosciences; Bio-Lyte 3/6 and 3/10 Ampholyte from Bio-Rad; and the Centriprep-30 concentrators from Amicon. All other reagents were of the highest grade available.

Methods

Growth Conditions and Preparation of Cytosolic and Membrane Extracts of Vegetative Cells—Axenic cultures of *Nostoc* PCC 7120 were grown photoautotrophically in BG-11 medium (10) at 35 °C for 1 week. During growth they were illuminated with cool white fluorescent light and bubbled with filtered air containing 1% (v/v) of CO_2. Filaments were harvested by centrifugation (4000 × *g*, 10 min, 4 °C), washed twice with Hepes-EDTA buffer (10 mM Hepes/NaOH, pH 7.4, 5 mM NaCl, 2 mM Na_2EDTA) and resuspended in the same buffer to a cell density of 80 μl/ml of packed cells. The suspension was made up to 20% (w/w) sucrose and 0.5% lysozyme, incubated at 37 °C for 2 h and centrifuged (3000 × *g*, 10 min, 4 °C). Thereafter, the pellet was resuspended in Hepes-EDTA buffer containing 0.0075% DNase I, incubated on ice for 30 min, passed twice through a precooled French pressure cell (Aminco) at 40 and 70 MPa, respectively, and centrifuged (5000 × *g*, 10 min, 4 °C). Then the supernatant was used to separate membrane vesicles and cytosolic components by ultracentrifugation (250,000 × *g*, 50 min, 4 °C) or adjusted to 42% (w/w) with solid sucrose for discontinuous density gradient centrifugation. This solution was overlaid with 35, 30, and 10% (w/w) sucrose in Hepes/NaOH buffer and centrifuged (Beckman SW-27 rotor, 131,500 × *g*, 16 h, 4 °C). The cytoplasmic membrane (orange layer) and thylakoid fractions (dark green layer) obtained by density gradient centrifugation were recentrifuged severalfold to reduce cross-contamination. All buffers contained 1 mM PMSF, 5 μM leupeptin, and 5 μM pepstatin A to reduce proteolytic degradation (11).

Preparation of Heterocyst Extracts—To obtain filaments containing heterocystous cells, *Nostoc* PCC 7120 was grown similar to that described above but using nitrogen-free BG-11 medium (10). Cyanobacterial cells were centrifuged (4000 × *g*, 10 min, room temperature), washed twice with 30 mM Hepes-Pipes-KOH buffer (with 10 mM Na_2EDTA, pH 7.2), suspended in 10 mM Hepes-KOH buffer (with 10 mM $MgCl_2$, 300 mM mannitol, 0.5% bovine serum albumin, 0.5% lysozyme, pH 7.2), and incubated at 35 °C for 1 h at a cell density of 50 μl of packed cells per ml. The lysozyme-treated cells were pelleted, washed twice with lysozyme-free mannitol buffer, resuspended in 30 mM Hepes-Pipes-KOH buffer (with 1 mM $MgCl_2$, 0.0075% DNase I, pH 7.2) to a cell density of 50 μl of packed cells per ml, and extruded through a precooled French pressure cell (Aminco) at 34.5 MPa and 4 °C. Unaffected heterocysts were separated from broken vegetative cells by centrifugation (4000 × *g*, 4 min, 4 °C) and disrupted by French Press extrusion at 138 MPa and 4 °C (6). The membranes and cytosolic components of heterocysts were separated as described for vegetative cells.

Electron Microscopy Combined with Immunogold Labeling—Samples of *Nostoc* PCC 7120 were agglutinated with a thrombin-fibrinogen solution, fixed with 3% glutaraldehyde (in 0.2 M phosphate buffer, pH 7.2) for 2 h, washed twice with 0.2 M phosphate buffer for 5 min, and post-fixed with 1% osmium tetroxide (in 0.2 M phosphate buffer, pH 7.2) for 2 h. Subsequently, samples were dehydrated by incubation in solutions of increasing ethanol and propylene oxide concentration and embedded in epoxy resin using resin-propylene oxide mixtures of increasing resin concentration. After drying at 40 °C for 2 h, the specimens were polymerized at 60 °C for 2 days. Ultrathin sections were produced using the Ultracut E ultramicrotome (Reichert-Jung) and mounted on 200-mesh nickel grids. The grids were treated with 5% H_2O_2 for 5 min, washed with PBS-T (PBS containing 0.1% Tween-20), and blocked with 5% bovine serum albumin (in PBS-T) for 30 min. The grids were incubated overnight in rabbit anti-FeSOD antibody, diluted 1:200 with 1% bovine serum albumin (in PBS-T), and washed three times with PBS-T for 15 min each. Incubation with goat anti-rabbit IgG antibody conjugated with 10-nm colloidal gold particles (diluted 1:20 with PBS-T) was performed for 1 h, the grids were washed twice with PBS-T, and twice with distilled water for 15 min each. Grids were poststained in 2% uranyl acetate for 15 min, washed in distilled water, incubated in lead citrate for 5 min, washed in distilled water, air-dried, and observed with a transmission electron microscope (CEM 902 from Zeiss) operating at 80 kV. Controls were made using preimmune serum instead of anti-FeSOD antibody (13, 14).

Cloning and Overexpression of FeSOD—DNA and protein sequence of the iron-containing superoxide dismutase was obtained from the CyanoBase, the genome data base for *Nostoc* PCC 7120, at www.kazusa.or.jp/cyano/Anabaena/. The following oligonucleotide primers were synthesized from geneXpress (Maria Wörth, Austria): primer 1 (5′-ATA CCA TGG CAT TTG TAC AGG AAC C-3′; 25 bases containing an NcoI restriction site), and primer 2 (5′-GTG CTC GAG AGC TTT AGC ATA ATT CGC-3′; 27 bases with a XhoI restriction site). Chromosomal DNA was obtained by treating *Nostoc* cell pellets with SDS and heat, followed by phenol/chloroform/isoamyl alcohol extraction and ethanol wash steps (15). To amplify the gene for FeSOD, primers 1 and 2, chromosomal DNA from *Nostoc* as the template and the TaKaRa ExTaq DNA polymerase were used for PCR under the following conditions: 94 °C for 2 min (hot start); 28 cycles at 92 °C for 30 s, 50 °C for 30 s and 72 °C for 1.5 min; finally at 72 °C for 10 min. The PCR product was fractionated on a 1% agarose gel, and the appropriate DNA was cut out and purified using the GFX PCR DNA and gel band purification kit. This DNA fragment was digested with the restriction enzymes NcoI and XhoI and cloned into the NcoI- and XhoI-digested, alkaline phosphatase-treated expression vector pET-28a(+) (16). The insert was sequenced by the dideoxy chain termination method (17). Competent *Escherichia coli* BL21(DE3) cells were transformed with the expression vector by electroporation (Gene Pulser, Bio-Rad), positive clones carrying the recombinant plasmid were selected and grown overnight on an orbital shaker (180 rpm) at 37 °C in LB medium containing 50 μg/ml kanamycin. M9ZB medium containing 50 μg/ml kanamycin and 100 μM $FeSO_4$ was inoculated with an overnight culture, shaken at 37 °C to reach an OD_{600} of 1.0 and induced by the addition of 1 mM isopropyl-1-thio-β-D-galactopyranoside. After 4 h of incubation at 37 °C, cells were harvested by centrifugation (5000 × *g*, 5 min, 4 °C), frozen, and stored at −80 °C until used. Cells were resuspended in lysis buffer (50 mM Tris/HCl, pH 8.0, containing 2 mM EDTA, 0.1% Triton X-100, 1 mM PMSF, 5 μM leupeptin, and 5 μM pepstatin A) and broken by sonication with short bursts. The cell extract was centrifuged (21,000 × *g*, 20 min, 4 °C), and from the supernatant the superoxide dismutase was purified.

Protein Purification—The supernatant was adjusted to 1 M NaCl and 20 mM imidazole and loaded on a chelating Sepharose column (1.6 × 10 cm) charged with 30 μmol of Zn^{2+}/ml gel and equilibrated with 67 mM phosphate buffer, pH 7.0, containing 1 M NaCl and 20 mM imidazole at 4 °C. The column was washed with 200 ml of the equilibration buffer, and bound proteins were eluted with 100 ml of a gradient of 20–500 mM imidazole in 67 mM phosphate buffer, pH 7.0, containing 1 M NaCl. The eluted proteins were concentrated with Centriprep concentrators. Proteins were loaded onto a Superdex 200 column equilibrated with 67 mM

Downloaded from http://www.jbc.org/ by guest on July 25, 2018

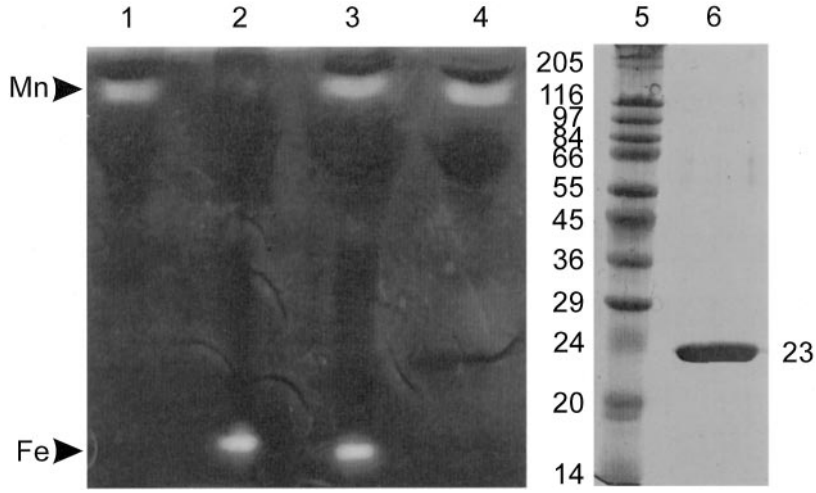

FIG. 1. **Gel electrophoresis of cell lysates and purified enzyme.** *Lanes 1–4*, nondenaturing PAGE of cell lysates from *Nostoc* PCC 7120 stained for SOD activity; *lane 1*, crude membranes; *lane 2*, cytosolic extract; *lane 3*, whole cell extract; *lane 4*, whole cell extract incubated with 10 mM hydrogen peroxide. The *upper band* represents the MnSOD and the *lower band* the FeSOD. *Lanes 5* and *6*, SDS-PAGE and Coomassie Blue staining; *lane 5*, molecular mass markers (molecular masses are given on the *left*); *lane 6*, purified FeSOD from *Nostoc* PCC 7120 overexpressed in *E. coli*.

phosphate buffer, pH 7.0, containing 150 mM KCl, at room temperature. Active fractions were concentrated using Centriprep concentrators, desalted with PD-10 columns, and stored frozen at −80 °C.

Molecular Mass Determination—The native molecular mass was determined by gel filtration chromatography and by nondenaturing gel electrophoresis. A Superdex 200 column was equilibrated with 67 mM phosphate buffer, pH 7.0, containing 150 mM KCl, and calibrated with standards including beef liver catalase (232 kDa), bovine serum albumin (67 kDa), chicken ovalbumin (43 kDa), and bovine carboanhydrase II (29 kDa). Native discontinuous gel electrophoresis at 7, 9, 11, and 13% acrylamide was employed to measure mobility in relation to the standards also used for gel filtration, and Ferguson plots were drawn to calculate molecular mass (18).

Polyacrylamide Gel Electrophoresis—SDS-PAGE was carried out on 15% slab gels as described by Laemmli (19) using SigmaMarkers and the Bio-Rad Mini-Protean II system. Proteins on the gel were stained with Coomassie Brilliant Blue. Detection of SOD activity was realized by combining native electrophoresis on 12% polyacrylamide gels with activity staining according to Beauchamp and Fridovich (20). This assay was also performed in the presence of azide, cyanide, or hydrogen peroxide to evaluate the sensitivity of the enzyme.

Isoelectric Focusing—Determination of the isoelectric point was done on 5% acrylamide gels containing Bio-Lyte ampholytes (pH 3–6 or 3–10) and using the Model 111 Mini IEF cell (Bio-Rad). Standard proteins were: amyloglucosidase (pI 3.6), trypsin inhibitor (pI 4.6), β-lactoglobulin (pI 5.1), carboanhydrase II (pI 5.9), carboanhydrase I (pI 6.6), myoglobin (pI 6.8/7.2).

Spectrophotometry—Spectrophotometric measurements were made on a Zeiss Specord S10 diode array or a Hitachi U-3000 spectrophotometer, both equipped with a thermostatted cell holder.

Activity Assay—SOD activity was determined by the ferricytochrome *c* assay (21), where xanthine and xanthine oxidase was used as the source of superoxide radicals and cytochrome *c* as the indicating scavenger of the radical. The assay mixture (3.0 ml) contained 50 mM phosphate buffer (pH 7.8), 0.1 mM EDTA, 50 μM xanthine, 20 μM cytochrome *c*, and 50 μl of buffer or sample solution of several dilutions. The absorbance at 550 nm was monitored with a spectrophotometer after the addition of 50 μl of a solution containing 0.2 units/ml xanthine oxidase and thermostatted at 25 °C. Under these conditions the reduction rate of cytochrome *c* was 0.0004 absorbance units per second in absence of SOD which corresponds to 2.1 nM s^{-1} cytochrome *c* reduced by one electron transfer from superoxide and is proportional to the superoxide concentration. SOD reduces the cytochrome *c* reduction rate, and a linear plot of reciprocal absorbance change per second *versus* protein concentration was used for computation of specific activity. One unit of SOD was defined as the amount of enzyme that inhibits the rate of cytochrome *c* reduction by 50% at pH 7.8 and 25 °C, calculated from the initial rate of reaction.

Determination of Protein Concentration—From cell extracts and partially purified SOD, the concentration was measured by the Coomassie Blue protein assay at 595 nm utilizing bovine serum albumin as a standard (22). The concentration of purified enzyme solutions was determined spectrophotometrically using the calculated molar absorbance coefficient ϵ_{280} = 46,410 M^{-1} cm^{-1} per subunit (23).

Sodium Azide Binding—The binding of azide to FeSOD was followed spectrophotometrically by increasing the NaN_3 concentration by stepwise addition of 5 μl of 0.2–5 M NaN_3 stock solutions to 1 ml of 100 μM FeSOD in 100 mM phosphate buffer, pH 7, and recording the spectrum.

Stopped Flow Measurements—To follow the reaction of superoxide and SOD the model SX-18MV stopped flow spectrophotometer from Applied Photophysics equipped with a 1-cm observation cell at room temperature was used. Calculation of kinetic parameters from experimental traces was performed with the SpectraKinetic work station v4.38 interfaced to the instrument. The superoxide solution was prepared in a glove box; 133 mg of potassium superoxide and 800 mg of 18-crown-6-ether were dissolved in 6.7 ml of dimethyl sulfoxide (Me_2SO), 3.3 ml dimethylformamide (DMF) and filtered. Both aprotic organic solvents were dried over a 3-Å molecular sieve. The sequential-mixing mode was utilized to follow the decrease of superoxide concentration. In the first step superoxide solution was mixed with 5 mM buffer at pH 10. After a delay time of 10 ms, this mixture was combined with buffer at pH 7–10 with or without the enzyme. The following molar absorbance coefficients were used for recording of the superoxide decay (wavelength is shown in parentheses): 2250 M^{-1} cm^{-1} (245 nm) and 284 M^{-1} cm^{-1} (300 nm) (24). Prior to data collection for superoxide decay, several shots of the buffer with Me_2SO/DMF mixture were used to determine the baseline. All stopped flow determinations were measured in 50 mM of final buffer concentration at various pH values between pH 7 and 10, containing 100 μM EDTA, and at least three determinations were performed per substrate and enzyme concentration.

Sequence Analysis—The amino acid sequences used in this work were extracted from the protein entries in the Entrez Protein search and retrieval system of NCBI (at www.ncbi.nlm.nih.gov:80/entrez/query.fcgi?db = Protein), which includes data from SwissProt, PIR, PRF, PDB, GenBank™, and RefSeq. Multiple sequence alignment was performed using ClustalX (25) and the following parameters: gap opening 10.0, gap extension 0.05 and the BLOSUM protein weight matrices. Phylogenetic analysis was performed using ClustalX, version 1.81, and the Bootstrap Neighbor Joining Tree option (25).

RESULTS

Detection of Superoxide Dismutase Activity in Nostoc PCC 7120—To search for enzymes that are able to destroy the superoxide radical anion, cultures of the filamentous cyanobacterium *Nostoc* PCC 7120 were grown under photoautotrophic conditions. Cells were broken, and one part was separated into a cytosolic and a membrane fraction. Because cyanobacteria possess two types of membrane, the membrane component was further separated into cytoplasmic and thylakoid membranes by density gradient centrifugation. The four cell extracts (whole cell extract, cytosol, cytoplasmic membranes, and thylakoids) were used for SOD activity assays and native gel electrophoresis combined with SOD-specific staining. Membrane-containing extracts were solubilized in 2% dodecyl maltoside before application to the native gel. After the electrophoretic run SOD staining of whole cell extracts showed two bands, which were interpreted as an indication of the presence of two different types of SOD (Fig. 1, *lane 1*). Separation of cytosol and membranes showed that the upper band is only

Downloaded from http://www.jbc.org/ by guest on July 25, 2018

TABLE I
Superoxide dismutase activities in cell extracts of vegetative cells and heterocysts of Anabaena PCC 7120

	Vegetative cells			Heterocysts	
	Cytosol	CM	ICM	Cytosol	CM + ICM
Stain on gel	+	+	+	+	+
Type of SOD	FeSOD	MnSOD	MnSOD	FeSOD	MnSOD
Spec.act.[a]	15.5	3.1	2.0	9.3	8.1

[a] Spec.act., specific activity in units per mg of protein determined with the ferrocytochrome *c* assay and using xanthine/xanthine oxidase as the superoxide radical-generating system.

present in membranes and the lower band only in the soluble cytosolic fraction (Fig. 1, *lane 2*). To determine the type of SOD, gels with electrophoresed whole cell extracts were incubated with 50 mM NaCN or 10 mM H_2O_2. Both bands were present with cyanide, indicating that they do not represent CuZnSOD, which is inhibited by cyanide. Hydrogen peroxide can be used to distinguish FeSOD and MnSOD because only FeSOD is inactivated by this reagent. With hydrogen peroxide, only the lower band disappeared. Therefore the upper band should be an MnSOD (bound to the membrane) and the lower band should be an FeSOD (within the cytosol). Quantitative measurements using the ferrocytochrome *c* assay gave the following values (specific activities in units per mg protein in parenthesis): cytosolic fraction (15.5 ± 2), cytoplasmic membrane (3.1 ± 0.5), and thylakoids (2.0 ± 0.7).

The next step was to show the presence and distribution of SODs in heterocysts. Therefore *Nostoc* PCC 7120 was grown in nitrogen-depleted medium and heterocysts were selectively separated from vegetative cells and broken. Whole heterocyst extracts also gave two bands at the same positions as vegetative cells in the native gel after SOD staining. Quantitative measurements using the ferrocytochrome *c* assay showed the following values (specific activities in units per mg protein in parenthesis): cytosolic fraction (9.3 ± 0.2), crude membranes (thylakoid and cytoplasmic membrane) (8.1 ± 0.5). Results for vegetative cells and heterocysts are summarized in Table I.

Localization of FeSOD in Nostoc PCC 7120 Cells by Immunogold Labeling—To determine the distribution of FeSOD in vegetative cells and heterocysts, an antibody raised against the *Anabaena cylindrica* FeSOD was used (13). SDS-PAGE and Western blotting had shown that the antibody did not cross-react with MnSOD and is specific for FeSOD. Ultrathin sections of filaments from *Nostoc* PCC 7120 grown under nitrogen-depleted conditions were incubated with this anti-FeSOD antibody and decorated with gold particles. FeSOD was present in both cell types and distributed throughout the cells. Fig. 2 depicts a gold-labeled and post-stained *Nostoc* heterocyst with the typical thick envelope. Quantitative analysis resulted in 5.3 gold particles per μm^2 within vegetative cells and 4.0 gold particles per μm^2 in heterocysts. Control experiments without antiserum gave no labeling. Also a significantly reduced amount of gold particles was seen when the preimmune serum was used. This confirmed that the gold particles bound to the antibody do reflect the presence of FeSOD. The even distribution of particles throughout the cell indicate a cytosolic occurrence of FeSOD in both cell types, heterocysts, and vegetative cells.

The Gene for the Iron-containing Superoxide Dismutase of Nostoc PCC 7120—Searching the entire genome of the cyanobacterium *Nostoc* PCC 7120 revealed two genes with high homology to superoxide dismutases. One of them (*sodA*) codes for a MnSOD. Analysis of the protein sequence showed that it contains a hydrophobic N terminus, which is responsible for membrane-anchoring (2). The second gene (*sodB*) encodes an iron-containing superoxide dismutase (FeSOD). Inspection of

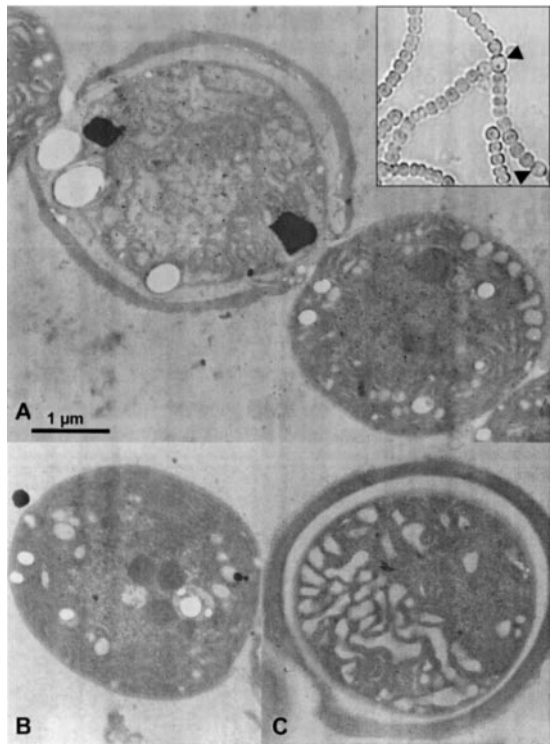

FIG. 2. **Electron microscopic immunogold labeling of FeSOD in vegetative cells and heterocysts from the filamentous cyanobacterium *Nostoc* PCC 7120.** Ultrathin sections of cyanobacterial cells were incubated overnight with polyclonal rabbit anti-FeSOD antibody (1:200 dilution) or preimmune serum. Cells were washed three times and incubated for 1 h with goat anti-rabbit IgG antibody-labeled colloidal gold (10 nm) and washed again four times. They were then stained with 2% uranyl acetate. *A*, immunogold labeling with anti-FeSOD antibody. In the *upper left* a heterocyst with its thick cell wall can be seen, and in the *lower right* a vegetative cell is present. The *inset* at the *upper right* shows a light micrograph of filaments from *Nostoc* PCC 7120 grown under nitrogen-depleted conditions. Two heterocysts are indicated with *arrowheads*. *B* and *C*, nonspecific immunogold labeling of a vegetative cell (*B*) and a heterocyst (*C*) using preimmune serum instead of anti-FeSOD antibody.

the amino acid sequence does not reveal any hydrophobic membrane anchor or signal sequence. Therefore, it should be a soluble cytosolic protein. The nucleotide sequence contains an open reading frame including 600 bp from the start site at ATG to the termination codon TAG, coding for a polypeptide chain of 200 amino acids.

Sequence Alignment and Phylogenetic Analysis—The *Nostoc* FeSOD was aligned with 42 additional FeSODs and three cambialistic SODs, mainly bacterial enzymes, but also including proteins from plant chloroplasts, archaebacteria, and unicellular eukaryotes. The amino acid sequence alignment of nine selected cyanobacterial FeSODs is shown in Fig. 3. Also aligned is the prototypical FeSOD from *E. coli*, where together with the *Thermosynechococcus elongatus* BP-1 FeSOD the three-dimensional structure is known. FeSODs are highly conserved throughout all kingdoms of life. The homology between *Nostoc* PCC 7120 FeSOD and various other FeSODs are as follows (values of percent identity and percent similarity are given in parentheses): *Nostoc commune* (87/94), *Nostoc punctiforme* (86/93), *Nostoc linckia* (83/90), *Plectonema boryanum* (77/84), *T. elongatus* (72/81), *Synechocystis* 6803 (60/72), *Synechococcus* 7942 (58/72), *Synechococcus* 6301 (57/71), *E. coli* (51/64). These homologies reflect the phylogenetic distance between the listed species; the phylogenetic tree constructed with ClustalX groups the cyanobacterial FeSODs within a separated cluster (Fig. 4). Filamentous cyanobacterial enzymes are combined in one sub-

Downloaded from http://www.jbc.org/ by guest on July 25, 2018

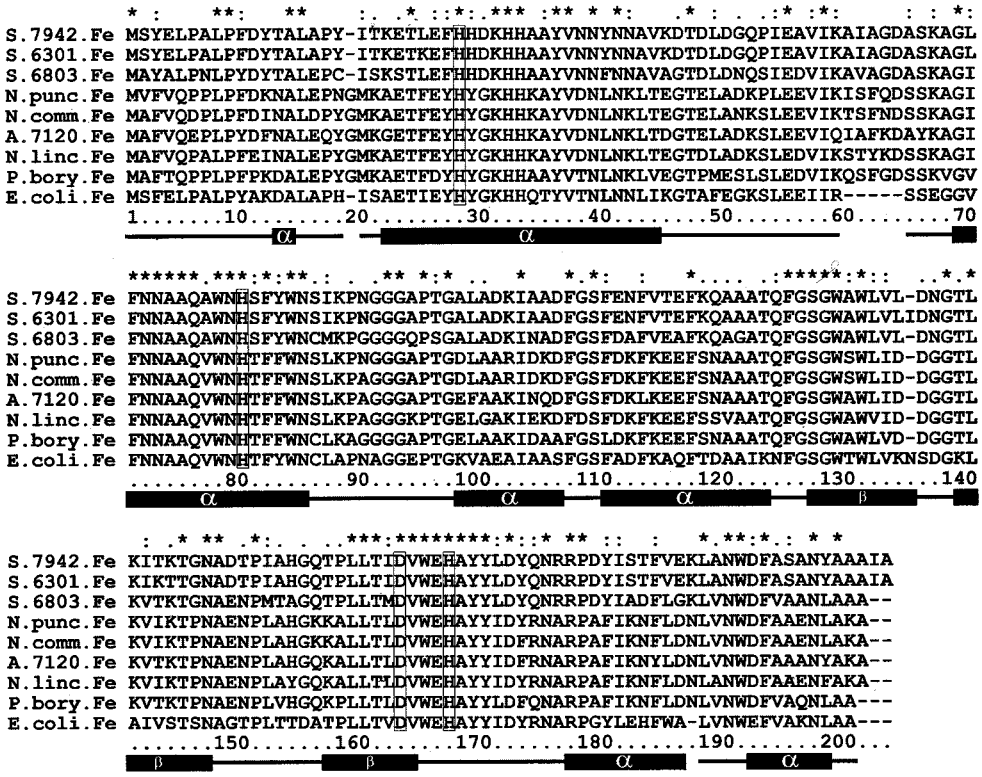

FIG. 3. **Amino acid sequence alignment of iron-containing superoxide dismutases from various cyanobacterial species and *E. coli*.** The protein sequences are aligned using the program ClustalX, version 1.81. The four amino acid residues coordinating the iron center are highlighted in *black*, residues involved in substrate entrance and hydrogen bond network are *boxed*. The *last line* depicts secondary structural elements (α-helices and β-strands) deduced from the three-dimensional structure of FeSOD from *E. coli*. Abbreviations: *Fe*, FeSOD; *A.7120*, *Nostoc* (*Anabaena*) PCC 7120; *N. comm.*, *N. commune*; *N. linc.*, *N. linckia*; *N. punc.*, *N. punctiforme*; *P. bory.*, *P. boryanum*; *S.6301*, *Synechococcus* PCC 6301; *S.6803*, *Synechocystis* PCC 6803; *S.7942*, *Synechococcus* PCC 7942; *T. elon.*, *T. elongatus* BP-1.

cluster and are about 80–90% identical. Unicellular are pooled in a second subcluster, which, interestingly, also includes the non-cyanobacterial, sulfur-reducing bacterium *Desulfovibrio vulgaris* FeSOD. The cambialistic SODs are spread within the FeSODs; therefore, they form no independent cluster and are separated from cyanobacterial FeSODs. Cambialistic SODs are enzymes with substantial catalytic activity either with iron or manganese in the active site. Until now no such cambialistic SOD was characterized in a cyanobacterium.

There are several amino acid residues that are highly conserved in all FeSODs and which are involved in ligand binding and/or the catalytic mechanism. Most important are four residues that coordinate the metal ion. In *Nostoc* FeSOD these are His-28, His-80, Asp-162, and His-166 (see Fig. 3), which normally form together with a hydroxide ion a trigonal bipyramidal coordination sphere. Also conserved are amino acids forming the substrate entrance (Trp-84, Tyr-36, His-32) and a hydrogen bond network (Gln-76, Tyr-36, Trp-129, Asn-79, Asp-162, His-32, Tyr-169) (26).

Expression in E. coli and Purification of Nostoc FeSOD—The *sodB* gene was amplified by PCR using appropriate primers and chromosomal *Nostoc* DNA and cloned into the expression vector pET-28a(+), which positions a hexahistidine at the C terminus. This construct was inserted into *E. coli* BL21(DE3). About 10 clones were screened for the presence of the *sodB* insert, and one was selected for overexpression. Sequencing of this clone confirmed the correct insertion of the gene. Expression of FeSOD and subsequent purification by metal-chelate affinity chromatography and gel filtration yielded ~100 mg of active enzyme per liter of *E. coli* culture. The yellow-orange color of the solution shows that an iron(III) is bound to the enzyme. The protein was stored in 5 mM phosphate buffer, pH 7, at −80 °C.

Absorption Spectroscopy of Nostoc 7120 FeSOD—Iron content was determined from the absorption spectrum using the peaks at 280 and 350 nm (see Fig. 5*A*). The peak at 280 nm corresponds to the content of aromatic amino acids, and from the sequence a molar absorbance coefficient ϵ_{280} of 46,410 M^{-1} cm^{-1} was calculated. The second characteristic peak of FeSOD is that of the iron at 350 nm with ϵ_{350} = 1850 M^{-1} cm^{-1} (27). Using the absorbances at these wavelengths from the spectrum, the iron occupancy of the recombinant enzyme was determined to be 0.98 Fe per subunit. Addition of 1 mM sodium dithionite to 200 μM recombinant enzyme led to the complete loss of the peak at 350 nm, showing the reduction of iron(III) to iron(II). After removal of the dithionite by gel filtration the catalytic activity was fully present.

Molecular Mass and Isoelectric Point of the FeSOD from Nostoc PCC 7120—All FeSODs characterized until now are homodimeric or homotetrameric proteins. To determine the oligomeric state of the *Nostoc* FeSOD, three methods were used. The first one was gel filtration chromatography on a Superdex 200 column, which showed that the purified recombinant protein has a mobility similar to that of chicken ovalbumin with 43 kDa. Nondenaturing polyacrylamide gel electrophoresis at several acrylamide concentrations combined with a Ferguson plot provided a native molecular mass of 42 kDa. Cross-linking with dimethyl suberimidate in Tris buffer at pH 9 and subsequent SDS-PAGE gave a band at 45 kDa. With these very similar results obtained by three different methods and the calculated molecular mass of the monomer of 23 kDa, also confirmed by SDS-PAGE without cross-linking (see Fig. 1, right side), the homodimeric nature of this FeSOD can be assumed.

Whereas for the wild-type SOD an isoelectric point (pI) of 5.14 was calculated using the amino acid sequence, the recom-

Downloaded from http://www.jbc.org/ by guest on July 25, 2018

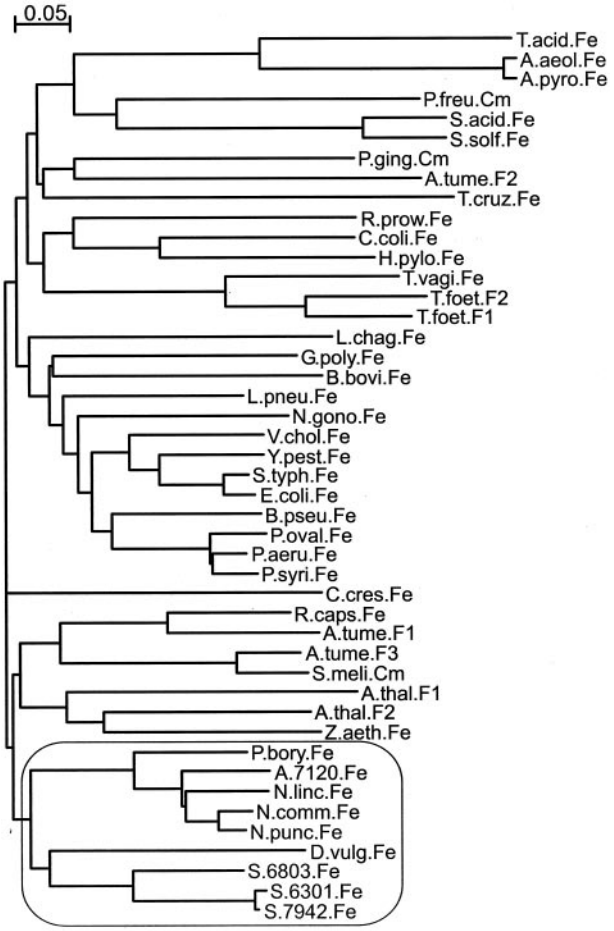

FIG. 4. **Phylogenetic relationships of iron-containing superoxide dismutases.** The phylogenetic tree was constructed using ClustalX, version 1.81, and the Bootstrap Neighbor Joining Tree option. Branch lengths represent calculated phylogenetic distances. The branch containing all cyanobacterial FeSODs is highlighted. Abbreviations: *Cm*, cambialistic SOD; *Fe*, F1-3, FeSODs; *A.7120*, *Nostoc* (*Anabaena*) PCC 7120; *A. aeol.*, *Aquifex aeolicus*; *A. pyro.*, *Aquifex pyrophilus*; *A. thal.*, *Arabidopsis thaliana*; *A. tume.*; *Agrobacterium tumefaciens*; *B. bovi.*, *Babesia bovis*; *B. pseu.*, *Burkholderia pseudomallei*; *C. coli.*, *Campylobacter coli*; *C. cres.*, *Caulobacter crescentus*; *D. vulg.*, *D. vulgaris*; *G. poly.*, *Gonyaulax polyedra*; *H. pylo.*, *Helicobacter pylori*; *L. chag.*, *Leishmania chagasi*; *L. pneu.*, *Legionella pneumophila*; *N. comm.*, *N. commune*; *N. gono.*, *Neisseria gonorrhoeae*; *N. linc.*, *N. linckia*; *N. punc.*, *N. punctiforme*; *P. aeru.*, *Pseudomonas aeruginosa*; *P. bory.*, *P. boryanum*; *P. freu.*, *Propionibacterium freudenreichii*; *P. ging.*, *Porphyromonas gingivalis*; *P. oval.*, *Pseudomonas ovalis*; *P. syri.*, *Pseudomonas syringae*; *R. caps.*, *Rhodobacter capsulatus*; *R. prow.*, *Rickettsia prowazekii*; *S.6301*, *Synechococcus* PCC 6301; *S.6803*, *Synechocystis* PCC 6803; *S.7942*, *Synechococcus* PCC 7942; *S. acid.*, *Sulfolobus acidocaldarius*; *S. meli.*, *Sinorhizobium meliloti*; *S. solf.*, *Sulfolobus solfataricus*; *S. typh.*, *Salmonella typhimurium*; *T. acid.*, *Thermoplasma acidophilum*; *T. cruz.*, *Trypanosoma cruzi*; *T. elon.*, *T. elongatus*; *T. foet.*, *Trichomonas fetus*; *T. vagi.*, *Trichomonas vaginalis*; *V. chol.*, *Vibrio cholerae*; *Y. pest.*, *Yersinia pestis*; *Z. aeth.*, *Zantedeschia aethiopica*.

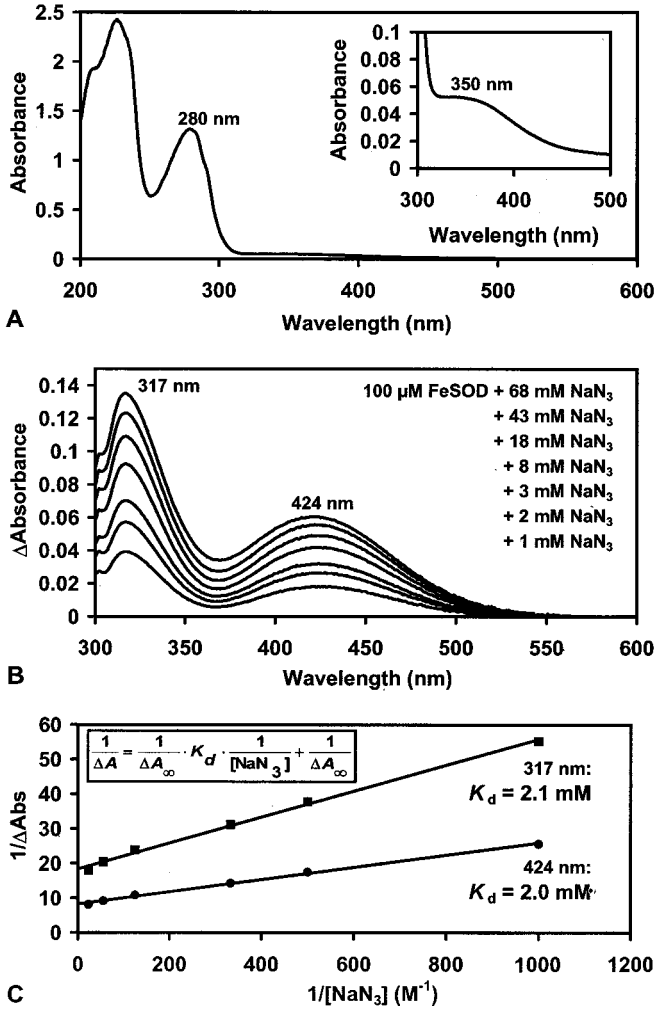

FIG. 5. **Spectra of recombinant *Nostoc* iron superoxide dismutase and its complex with azide.** *A*, UV/vis absorption spectrum of 28 μM FeSOD. The *inset* shows a magnification of the iron-specific peak at 350 nm. *B*, difference spectra produced by mixing oxidized FeSOD with increasing azide concentrations. Oxidized FeSOD without any azide was used as the reference spectrum. *C*, double-reciprocal plot of absorbance difference (ΔA) *versus* azide concentration (NaN_3) to calculate the dissociation constant (K_d) of the complex of FeSOD with azide. The formula used for the calculation of K_d is shown in the *inset*. All spectra were recorded at room temperature in 100 mM phosphate buffer, pH 7.0.

binant enzyme with a C-terminal hexahistidine tag gave a pI of 5.77. Isoelectric focusing of the purified recombinant FeSOD confirmed the calculated pI with a value of pI 5.9 showing that it is an acidic protein.

Activity Measurements of Recombinant FeSOD—Catalytic activity was determined by the ferricytochrome *c* assay using xanthine and xanthine oxidase as source of superoxide. The specific activity was (2040 ± 90) units mg^{-1} at pH 7.8. Incubation of 100 μM recombinant enzyme with 10 mM H_2O_2, NaCN, or NaN_3 for 30 min and thereafter performing the activity assay led to distinct results. No inhibition was detectable with cyanide, whereas azide reduced the activity by 30%. Hydrogen peroxide led to the complete loss of activity. Removing the H_2O_2 by gel filtration does not restore the activity, which shows irreversible inactivation of FeSOD (28). Similar results were obtained on a nondenaturing PAGE. 5 μg of FeSOD were loaded per lane and electrophoresed. After incubation with 10 mM H_2O_2, 50 mM NaN_3, or 50 mM NaCN, respectively, the gel was stained with nitro blue tetrazolium (20). With cyanide a band was visible on a blue background, but azide and hydrogen peroxide led to a complete disappearance of bands that have SOD activity. These measurements showed the typical behavior of a FeSOD.

Several anions act as competitive inhibitors of FeSODs, which can be grouped into two classes according to their ability to change the iron peak at 350 nm (24). Spectral changes were analyzed by mixing 1 ml of 28 μM recombinant *Nostoc* FeSOD with 25 μl 2 M Na_2SO_4, NaCl, KSCN, HCOONa, NaF, or NaN_3 (50 mM final concentration of anion) after recording the spectrum of free FeSOD. Sulfate, chloride, thiocyanate, and formate inhibit FeSOD activity but do not change the spectral

Downloaded from http://www.jbc.org/ by guest on July 25, 2018

properties of FeSOD. This is interpreted as an indication that the anion does not directly bind to the metal ion but blocks the access of superoxide to the active site. However fluoride led to disappearance of the iron peak, whereas azide gave rise to two new bands in the visible region (see Fig. 5*B*), which showed that these two anions directly bind to the iron of the enzyme. To measure the dissociation constant for the complex between the *Nostoc* FeSOD and azide, 100 μM enzyme was titrated by increasing the NaN_3 concentration from 1 to 68 mM in 100 phosphate buffer at pH 7.0, and absorption spectra were recorded (Fig. 5, *B* and *C*). The dissociation constant (K_d) was calculated from the difference spectra of cyanide complex minus oxidized FeSOD and showed a value of K_d = 2.1 mM. This value is very similar to the K_d determined for the FeSOD of *E. coli*, which gave K_d = 2.3 mM (24).

Stopped Flow Measurements—Stopped flow technology was used to quantitate steady-state SOD activity at 15 or 20 °C and pH values between pH 7 and 10. Two different final superoxide concentrations (220 μM and 4.6 mM) were employed to follow uncatalyzed and SOD-catalyzed superoxide decay. The solubility of the potassium superoxide (KO_2) in the Me_2SO:DMF mixture was increased by utilizing crown ethers. The amount of organic solvent in the final mixture was reduced to 5% (v/v) by first mixing superoxide solution in Me_2SO:DMF with a weak buffer at pH 10 in a 1:10 ratio. The resulting solution was combined with a strong buffer of the desired pH in a second mixer. High quality chemicals guaranteed second-order self-dismutation in the absence of enzyme at pH 7–10 as could be seen from a linear fit of reciprocal superoxide concentration *versus* time. To monitor enzyme kinetics the concentrations of recombinant *Nostoc* FeSOD were varied between 12.5 nM (lowest concentration at pH 7) and 20 μM (highest concentration at pH 10). Measurements at low and high superoxide concentrations with FeSOD showed no indication of saturation. From these curves it was not possible to calculate turnover numbers and Michaelis constants (K_m) using the model described by Bull and Fee (24, 29). Our equipment did not reach temperatures as low as 3 °C or 5.5 °C which were used to measure superoxide decay with *E. coli* FeSOD or bovine CuZnSOD to demonstrate a rate-limiting first-order process and calculate turnover numbers and K_m (24, 29). But the curves fit very well by a first-order superoxide decay and a plot of the logarithm of absorbance *versus* time is linear. This is similar to the behavior of bovine CuZnSOD at 20 °C (29, 30). At constant superoxide concentrations, the enzyme was varied from nanomolar to micromolar concentrations (Fig. 6*A*) and the obtained pseudo-first-order rate constants (k_{obs}) were plotted against concentration. The plots were linear over the enzyme concentration range confirming that the reaction is first-order in enzyme concentration (Fig. 6*B*). The contribution to the observed rate by the second-order self-dismutation is small (see intercept in Fig. 5*B*) under the conditions of the experiment over the pH 7–10. The slope of the k_{obs} *versus* enzyme concentration plot allowed the calculation of the second-order rate constant (k). These second-order rate constants decrease with increasing pH value by a factor of about ten per pH unit (Fig. 6*C*), $k = 5.3 \times 10^9$ M^{-1} s^{-1} (pH 7), 1.7×10^8 M^{-1} s^{-1} (pH 8), 3.9×10^7 M^{-1} s^{-1} (pH 9), 4.8×10^6 M^{-1} s^{-1} (pH 10). This is in accordance with other FeSODs and MnSODs, which also show reciprocal pH dependence and is in contrast to the pH independence of CuZnSOD over the range 7–9 (30).

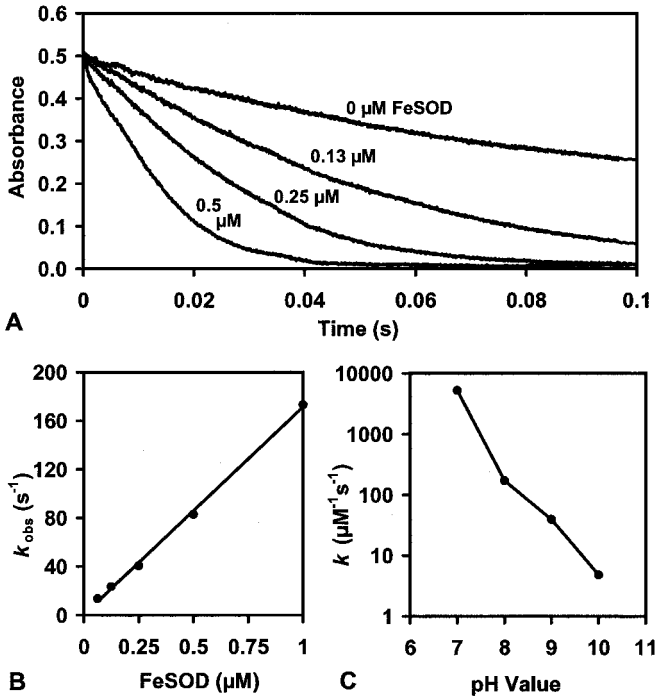

FIG. 6. **Stopped flow measurements of recombinant *Nostoc* FeSOD.** *A*, stopped flow time traces at various FeSOD concentrations with 220 μM superoxide recorded at 245 nm and 20 °C in 50 mM phosphate buffer, pH 8. *B*, pseudo-first-order rate constants (k_{obs}) of superoxide plotted against the FeSOD concentration. *C*, effect of pH on the rate constants (k) of the reaction of FeSOD and superoxide.

DISCUSSION

Cyanobacteria form a diverse group of bacteria that use oxygenic photosynthesis for energy production from sunlight. Many cyanobacteria are able to reduce atmospheric dinitrogen to ammonia by an enzyme called nitrogenase. In some filamentous cyanobacteria, nitrogen-fixing heterocysts are formed. These heterocysts are terminally differentiated cells with thick cell walls whose interior becomes nearly anaerobic, mainly as a consequence of respiration, allowing the oxygen-sensitive process of nitrogen fixation to continue (31). Nitrogenase is highly sensitive to dioxygen and is irreversibly inactivated by it. Organisms able to perform N_2 fixation in aerobiosis have evolved mechanisms to protect this nitrogenase from the deleterious effects of O_2. Reactive oxygen species produced from O_2 may be involved in these toxic reactions (32). Superoxide directly reacts with iron-sulfur clusters in enzymes, such as aconitase, containing 4Fe-4S clusters. Thereby, the enzyme is inactivated by releasing iron from the cluster (33). It is tempting to speculate that a similar mechanism could be responsible for irreversible inactivation of nitrogenase reductase and/or nitrogenase through the destruction of their iron-sulfur clusters. Reactive oxygen species may also change the redox state of the 4Fe-4S clusters, thus inhibiting the acceptance or donation of electrons (4). Therefore, in a nitrogen-fixing cyanobacterium it is extremely important to control the level of oxygen and reactive oxygen molecules (4). This is underscored by the recent investigations of the proteome of *N. punctiforme* (35), where the cells were grown in nitrogen-deficient media, and a cytosolic fraction was analyzed by two-dimensional electrophoresis and mass spectrometry. Based on optical density from the two-dimensional gel, FeSOD was shown to be the most abundant non-phycobiliprotein found in the cytosolic extract. In addition three putative peroxidases with homology to peroxiredoxins were shown to also belong to the most highly expressed proteins of this filamentous nitrogen-fixing cyanobacterium (35). These findings clearly emphasize the importance of free radical management in cyanobacteria.

Nostoc PCC 7120 possesses two types of superoxide dismutase, a soluble FeSOD in the cytosol and one and the same membrane-bound MnSOD in both membrane types. The solu-

Downloaded from http://www.jbc.org/ by guest on July 25, 2018

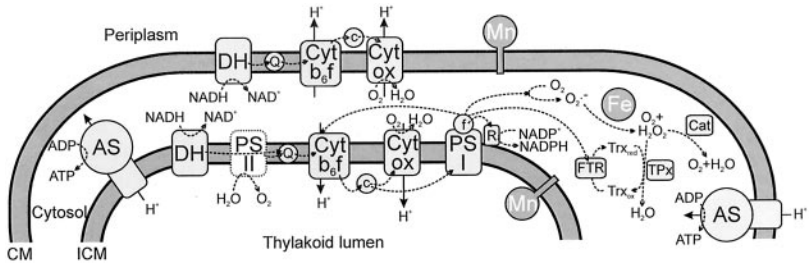

FIG. 7. **Scheme of electron transport processes of photosynthesis and respiration in vegetative cells and heterocysts of a filamentous cyanobacterium including localization of Fe- and Mn-containing superoxide dismutases and the water-water cycle.** Electron transfer pathways between the complexes of photosynthesis and respiration are illustrated by *broken lines*. In heterocysts the oxygen-evolving photosystem II is not present. Abbreviations: *PSI*, PSII, photosystems I and II; *Q*, plastoquinone; *f*, ferredoxin; *R*, ferredoxin-NADP$^+$ reductase; *c*, soluble cytochrome c_{554} or plastocyanin; *DH*, either bacteria-like nonproton-translocating one-subunit NADH dehydrogenase or mitochondria-like multisubunit NADH dehydrogenase; *Cyt* b_6f, cytochrome b_6f complex; *Cyt ox*, cytochrome *c* oxidase; *AS*, ATP synthase; *Fe* or *Mn*, iron- or manganese-containing superoxide dismutase; *Cat*, catalase or catalase-peroxidase; *TPx*, thioredoxin peroxidase; Trx_{red} and Trx_{ox}, reduced and oxidized thioredoxin; *FTR*, ferredoxin-thioredoxin reductase.

ble FeSOD has a 5–8-fold higher specific activity than that of cytoplasmic or thylakoid membranes, respectively. Topology analysis of the MnSOD predicts that the catalytic domain is pointing outwards, in the case of a cyanobacterium meaning to the periplasm or the thylakoid lumen (2). Fig. 7 schematically depicts the different compartments of a cyanobacterial cell including the electron transport components of photosynthesis and respiration, which are the main source of superoxide production. The chlorophyll-free cytoplasmic membrane contains only the respiratory machinery whereas thylakoid membranes possess both systems. Additionally the localization of the two SODs is also illustrated. Because most of the superoxide radicals are produced at the iron-sulfur clusters of photosystem I on the cytosolic site, FeSOD seems to be more important to keep the superoxide level low. But also the thylakoid lumen may contain superoxide, and an additional SOD is necessary to remove it in this compartment. In particular, cyanobacterial membranes have a high content of polyunsaturated fatty acids (36), so the concentration of reactive oxygen species should be low to prevent oxidative damage. The membrane-bound MnSOD could play this important role in thylakoid lumen and periplasm.

From plant chloroplasts it is known that the stromal superoxide dismutase is an important component of a system that scavenges reactive oxygen species and dissipates excess photons, the water-water cycle (37, 38). At high light intensities, low CO_2 concentrations, or other stress conditions, electrons formed in photosystem II from water are used for photoreduction of dioxygen in photosystem I. The superoxide radical formed is rapidly converted to hydrogen peroxide, which can be detoxified by ascorbate peroxidase providing water. The resulting oxidized forms of ascorbate are re-reduced by ferredoxin, monodehydroascorbate reductase, or dehydroascorbate reductase (37, 38).

Analogous to plant chloroplasts, the water-water cycle also functions in cyanobacteria (39). The FeSOD at the cytosolic site of the thylakoid membranes of *Nostoc* PCC 7120 and many other cyanobacteria removes superoxide at the production site at photosystem I. But the scavenging of hydrogen peroxide is different in cyanobacteria compared with chloroplasts. Cyanobacteria do not contain an ascorbate peroxidase, but they use catalase and/or thioredoxin peroxidase (2-cysteine peroxiredoxin) activities to remove H_2O_2 (40). In the catalase reaction, catalase peroxidase (or classical, monofunctional catalase) is utilized to disproportionate H_2O_2 without the need of any electron donor. In the second type thioredoxin peroxidase reduces H_2O_2 to water using reduced thioredoxin, which is regenerated via ferredoxin-thioredoxin reductase by electrons from photosystem I (39). In the genome of *Nostoc* PCC 7120 one gene for manganese-containing catalase (61% sequence identity to that of *Bacillus halodurans*), one gene for thioredoxin peroxidase and two genes for 1-cysteine peroxiredoxin can be found (40). Therefore, both types of H_2O_2 removal systems could be used in the water-water cycle of *Nostoc* PCC 7120 (Fig. 7).

The water-water cycle (including the FeSOD) fulfills several physiological functions. It keeps the concentration of photoproduced reactive oxygen species low and prevents the generation of hydroxyl radicals. At high light intensities this cycle can also prevent the over-reduction of electron carriers (which leads to photoinhibition) by working as an alternative photon and electron sink (38). The electron flux produced through the water-water cycle delivers ATP for the formation of an inorganic carbon pool within the cell and for the CO_2 fixation in the Calvin-Benson cycle (39).

What is known about the distribution and function of both SODs in heterocysts of *Nostoc* PCC 7120? Separation of heterocystous cytosol from total membranes clearly depicts that both fractions contain SOD activity to a similar extent (see Table I) and that the FeSOD is again in the cytosol and MnSOD membrane-bound. This is in contrast to a previous article (9) where the authors agree with our group that the FeSOD is soluble and the MnSOD is membrane-bound and both SODs are present in vegetative cells; although in heterocysts they could only detect the FeSOD. The reason for this difference may perhaps lie in deviations of the exact growth conditions. They described that FeSOD increased within the first few hours of induction of heterocyst formation, remained at a high level until heterocyst differentiation was complete, and thereafter declined to normal levels. The increased expression of FeSOD during the phase of heterocyst differentiation corresponds to the high energy need during this phase, which is always correlated with an increased oxygen metabolism. The MnSOD was only elevated during periods of high oxidative stress (9). Therefore, the FeSOD could be more important for *Nostoc* PCC 7120 under nitrogen-depleted conditions where growth is dependent on heterocyst formation and nitrogenase activity.

Are the investigations in *Nostoc* PCC 7120 relevant for superoxide detoxification in other cyanobacteria? Which superoxide dismutases are present in other cyanobacteria? To answer these questions we looked into data bases of completely or partially sequenced cyanobacteria of different habitats to detect genes, which could code for superoxide dismutases (see Table II). Until now there were only a few reports describing the appearance of SODs in cyanobacteria, *e.g.* in 1975 the presence of an FeSOD and an MnSOD was reported in *P. boryanum* (41). FeSOD was localized in the cytosol and MnSOD in the thylakoids in three cyanobacterial species (42). Superoxide dismutase activity was also measured in vegetative

Downloaded from http://www.jbc.org/ by guest on July 25, 2018

TABLE II

Genes of superoxide dismutase in 13 cyanobacterial strains including the putative localization of proteins (deduced from the amino acid sequence)

In parentheses below the strain names their habitat, manifestation, formation of heterocysts, and content of nitrogenase genes are listed. Protein sequences are from www.kazusa.or.jp/cyano/cyano.html and from www.jgi.doc.gov/JGImicrobial/html/index.html. Localization was determined with the PSORT program, version 6.4, at http://psort.nibb.ac.jp/form.html (34).

Cyanobacterium	Superoxide dismutase (gene number)	Putative localization
Anabaena (Nostoc) PCC 7120	FeSOD (alr2938)	Cytosol
(freshwater, filamentous, with heterocysts, with nitrogenase)	MnSOD (all0070)	Membrane-bound
Anabaena variabilis ATCC 29413	FeSOD (gene 218.395)	Cytosol
(freshwater, filamentous, with heterocysts, with nitrogenase)	MnSOD (gene 257.5591)	Membrane-bound
N. punctiforme ATCC 29133	FeSOD (gene 461.70)	Cytosol
(freshwater, filamentous, with heterocysts, with nitrogenase)	MnSOD (gene 458.34)	Membrane-bound
	MnSOD (gene 507.217)	Membrane-bound
P. boryanum UTEX 485	FeSOD (*sodB*)	Cytosol
(freshwater, filamentous, no heterocysts, with nitrogenase)	MnSOD (*sodA1*)	Membrane-bound
	MnSOD (*sodA2*)	Cytosol
	MnSOD (*sodA3*)	Incomplete sequence
Trichodesmium erythraeum	NiSOD (gene 6285)	Cytosol
(marine, filamentous, no heterocysts, with nitrogenase)	MnSOD (gene 7063)	Membrane-bound
G. violaceus PCC 7421	FeSOD (glr4327)	Cytosol
(freshwater, unicellular, no nitrogenase)	MnSOD (gll0682)	Membrane-bound
	CuZnSOD (glr1981)	Cytosol
	CuZnSOD (glr2170)	Cytosol
Synechocystis PCC 6803	FeSOD (slr1516)	Cytosol
(freshwater, unicellular, no nitrogenase)		
Synechococcus elongatus PCC 7942	FeSOD (gene 132.996)	Cytosol
(freshwater, unicellular, no nitrogenase)		
T. elongatus BP-1	FeSOD (tll1519)	Cytosol
(freshwater, unicellular, no nitrogenase)	MnSOD (tlr0036)	Membrane-bound
Synechococcus WH8102	NiSOD (SYNW1626)	Cytosol
(marine, unicellular, no nitrogenase)		
Prochlorococcus marinus MED4	NiSOD (PMM1294)	Cytosol
(marine, unicellular, no nitrogenase)		
P. marinus MIT9313	NiSOD (PMT0340)	Cytosol
(marine, unicellular, no nitrogenase)		
P. marinus SS120	NiSOD (Pro1368)	Cytosol
(marine, unicellular, no nitrogenase)		

cells and heterocysts of *A. cylindrica*, with heterocysts having lower levels of activity (43). Four genes of SOD, one coding for an FeSOD and three coding for MnSOD, were characterized in *P. boryanum* (44). As well a CuZnSOD was identified in the marine cyanobacterium *Synechococcus* WH7803 (45). X-ray crystallography was performed for the FeSOD of *T. elongatus* (46) and the MnSOD of *Nostoc* PCC 7120 (8).

Table II lists twelve cyanobacterial species or strains where sequences of the whole or nearly complete genome are available. Included are also data from *P. boryanum* (44). All filamentous cyanobacteria seem to contain a membrane-bound MnSOD, whereas unicellular cyanobacteria only have a cytosolic superoxide dismutase with the exception of *Gloeobacter violaceus* and *T. elongatus*, which also have a membrane-bound MnSOD. What is especially interesting, is the fact that all freshwater cyanobacteria contain a cytosolic FeSOD, but marine cyanobacteria do not comprise a gene for FeSOD; however, they encode a protein with 30–40% identity and 50–60% similarity to NiSOD of *Streptomyces* species (12). This may be related to the very low content of dissolved iron in upper layers of the open ocean. To summarize, all cyanobacteria contain a cytosolic SOD, which contain iron (freshwater cyanobacteria) or nickel (marine cyanobacteria) at the active site and could be the housekeeping superoxide dismutase. Some cyanobacteria have additional SODs, in particular filamentous species with nitrogenase activity appear to need one or more supplementary membrane-bound MnSODs to effectively lower superoxide concentration.

REFERENCES

1. Peschek, G. A., Obinger, C., and Paumann, M. (2004) *Physiol. Plant* **120,** 358–369
2. Regelsberger, G., Atzenhofer, W., Rüker, F., Peschek, G. A., Jakopitsch, C., Paumann, M., Furtmüller, P. G., and Obinger, C. (2002) *J. Biol. Chem.* **277,** 43615–43622
3. Golden, J. W., and Yoon, H. S. (1998) *Curr. Opin. Microbiol.* **1,** 623–629
4. Fay, P. (1992) *Microbiol. Rev.* **56,** 340–373
5. Walsby, A. E. (1985) *Proc. R. Soc. Lond. B.* **226,** 345–366
6. Wastyn, M., Achatz, A., Molitor, V., and Peschek, G. A. (1988) *Biochim. Biophys. Acta* **935,** 217–224
7. Berman-Frank, I., Lundgren, P., Chen, Y.-B., Küpper, H., Kolber, Z., Bergmann, B., and Falkowski, P. (2001) *Science* **294,** 1534–1537
8. Atzenhofer, W., Regelsberger, G., Jacob, U., Peschek, G. A., Furtmüller, P. G., Huber, R., and Obinger, C. (2002) *J. Mol. Biol.* **321,** 479–489
9. Li, T., Huang, X., Zhou, R., Liu, Y., Li, B., Nomura, C., and Zhao, J. (2002) *J. Bacteriol.* **184,** 5096–5103
10. Stanier, R. Y., Kunisawa, R., Mandel, M., and Cohen-Bazire, G. (1971) *Bacteriol. Rev.* **35,** 171–205
11. Peschek, G. A., Wastyn, M., Trnka, M., Molitor, V., Fry, I. V., and Packer, L. (1989) *Biochemistry* **28,** 3057–3063
12. Youn, H. D., Kim, E. J., Roe, J. H., Hah, Y. C., and Kang, S. O. (1996) *Biochem. J.* **318,** 889–896
13. Canini, A., Civitareale, P., Marini, S., Grilli Caiola, M., and Rotilio G. (1992) *Planta* **187,** 438–444
14. Maunsbach, A. B. (1998) in *Cell Biology, A Laboratory Handbook* (Celis, J. E., ed) Vol. 3, pp. 249–276, Academic Press, San Diego
15. Williams, J. G. K. (1988) *Methods Enzymol.* **167,** 766–778
16. Studier, W., Rosenberg, A. H., Dunn, J. J., and Dubendorff, J. W. (1990) *Methods Enzymol.* **185,** 60–89
17. Sanger, F., Nicklen, S., and Coulson, A. R. (1977) *Proc. Natl. Acad. Sci. U. S. A.* **74,** 5463–5467
18. Gallagher, S. R. (1995) in *Current Protocols in Protein Science* (Coligan, J. E., Dunn, B. M., Speicher, D. W., and Wingfield, P. T., eds) pp. 10.3.1–10.3.11, John Wiley & Sons, New York
19. Laemmli, U. K. (1970) *Nature* **227,** 680–685
20. Beauchamp, C., and Fridovich, I. (1971) *Anal. Biochem.* **44,** 276–287
21. McCord, J. M., and Fridovich, I. (1969) *J. Biol. Chem.* **244,** 6049–6055
22. Bradford, M. M. (1976) *Anal. Biochem.* **72,** 248–254
23. Pace, C. N., Vajdos, F., Fee, L., Grimsley, G., and Gray, T. (1995) *Protein Sci.* **4,** 2411–2423
24. Bull, C., and Fee, J. A. (1985) *J. Am. Chem. Soc.* **107,** 3295–3304
25. Jeanmougin, F., Thompson, J. D., Gouy, M., Higgins, M., and Gibson, T. J. (1998) *Trends Biochem. Sci.* **23,** 403–405
26. Miller, A.-F. (2001) in *Handbook of Metalloproteins* (Messerschmidt, A., Huber, R., Poulos, T., and Wieghardt, K., eds) Vol. 2, pp. 668–682, Wiley, New York
27. Slykhouse, T. O., and Fee, J. A. (1976) *J. Biol. Chem.* **251,** 5472–5477
28. Beyer, W. F., and Fridovich, I. (1987) *Biochemistry* **26,** 1251–1257
29. Fee, J. A., and Bull, C. (1986) *J. Biol. Chem.* **261,** 13000–13005

Downloaded from http://www.jbc.org/ by guest on July 25, 2018

30. Riley, D. P., Rivers, W. J., and Weiss, R. H. (1991) *Anal. Biochem.* **196,** 344–349
31. Böhme H. (1998) *Trends Plant Sci.* **3,** 346–351
32. Bagchi, S. N., Ernst, A., and Böger, P. (1991) *Z. Naturforsch.* **46c,** 407–415
33. Flint D. H., and Allen R. M. (1996) *Chem. Rev.* **96,** 2315–2334
34. Nakai, K., and Horton, P. (1999) *Trends Biochem. Sci.* **24,** 34–35
35. Hunsucker, S. W., Klage, K., Slaughter, S. M., Potts, M., and Helm, R. F. (2004) *Biochem. Biophys. Res. Commun.* **317,** 1121–1127
36. Vargas, M. A., Rodriguez, H., Moreno, J., Olivares, H., Del Campo, J. A., Rivas, J., and Guerrero, M. G. (1998) *J. Phycol.* **34,** 812–817
37. Asada, K. (1999) *Annu. Rev. Plant Physiol. Plant Mol. Biol.* **50,** 601–639
38. Asada, K. (2000) *Phil. Trans. R. Soc. Lond. B.* **355,** 1419–1431
39. Miyake, C., and Asada, K. (2003) in *Photosynthesis in Algae* (Larkum, A. W., Douglas, S. E., and Raven, J. A., eds) pp. 183–204, Kluwer Academic Publishers, The Netherlands
40. Regelsberger, G., Jakopitsch, C., Plasser, L., Schwaiger, H., Furtmüller, P. G., Peschek, G. A., Zamocky, M., and Obinger, C. (2002) *Plant Physiol. Biochem.* **40,** 479–490
41. Asada, K., Yoshikawa, K., Takahashi, M., Maeda, Y., and Enmanji, K. (1975) *J. Biol. Chem.* **250,** 2801–2807
42. Okada, S., Kanematsu, S., and Asada, A. (1979) *FEBS Lett.* **103,** 106–110
43. Henry, L. E. A., Gogotov, I. N., and Hall, D. O. (1978) *Biochem. J.* **174,** 373–377
44. Campell, W. S., and Laudenbach, D. E. (1995) *J. Bacteriol.* **177,** 964–972
45. Chadd, H. E., Newman, J., Mann, N. H., and Carr, N. G. (1996) *FEMS Microbiol. Lett.* **138,** 161–165
46. Kerfeld, C. A., Yoshida, S., Tran, K. T., Yeates, T. O., Cascio, D., Bottin, H., Berthomieu, C., Sugiura, M., and Boussac, A. (2003) *J. Biol. Inorg. Chem.* **8,** 707–714

Downloaded from http://www.jbc.org/ by guest on July 25, 2018

The Iron Superoxide Dismutase from the Filamentous Cyanobacterium *Nostoc* PCC 7120: LOCALIZATION, OVEREXPRESSION, AND BIOCHEMICAL CHARACTERIZATION

Günther Regelsberger, Ulrike Laaha, Dagmar Dietmann, Florian Rüker, Antonella Canini, Maria Grilli-Caiola, Paul Georg Furtmüller, Christa Jakopitsch, Günter A. Peschek and Christian Obinger

J. Biol. Chem. 2004, 279:44384-44393.
doi: 10.1074/jbc.M406254200 originally published online August 9, 2004

Access the most updated version of this article at doi: 10.1074/jbc.M406254200

Alerts:
- When this article is cited
- When a correction for this article is posted

Click here to choose from all of JBC's e-mail alerts

This article cites 42 references, 14 of which can be accessed free at
http://www.jbc.org/content/279/43/44384.full.html#ref-list-1

Downloaded from http://www.jbc.org/ by guest on July 25, 2018